

ANALYSIS OF THE QUASIDIFFUSION METHOD ON TWO-DIMENSIONAL PROBLEMS WITH SPATIALLY PERIODIC MEDIA

Adrian Constantinescu* and Dmitriy Y. Anistratov

Department of Nuclear Engineering

North Carolina State University

Raleigh, NC 27695-7909

acconsta@unity.ncsu.edu; anistratov@ncsu.edu

ABSTRACT

We study convergence of the quasidiffusion (QD) method on two-dimensional spatially periodic problems with strong heterogeneities. A Fourier analysis of the linearized QD equations in the vicinity of the solution is performed. The analysis shows that in Periodic Horizontal Interface (PHI) problems the QD iteration method loses its effectiveness and even diverges in some cases. Numerical results of finite-medium PHI problems are presented to demonstrate the behavior of the QD method that was theoretically predicted.

Key Words: particle transport equation, iteration methods, Fourier analysis

1. INTRODUCTION

Recent research on transport acceleration methods showed that some of them lose their effectiveness in problems with strongly heterogeneous media [1–4]. The diffusion synthetic acceleration (DSA) and transport synthetic acceleration (TSA) methods has been studied by means of a Fourier analysis on problems with spatially periodic media. It enabled one to find out details of effects of material discontinuity on convergence behavior of these iterative methods.

In this paper, we analyze the convergence of the quasidiffusion (QD) method [5] for this class of transport problems in 2D geometry. The QD method is a nonlinear iteration method and hence the Fourier analysis cannot be directly applied to study its properties. The QD equations must be linearized about the solution. Then the analysis of the convergence of the method is performed in the vicinity of the solution. In case of a special problem with an infinite uniform medium and constant source, the analytic solution is known [6]. However, in heterogeneous-medium problems this is not the case.

We use an approach for stability analysis of nonlinear transport iteration methods for infinite medium problems with spatially periodic material composition that was developed and applied to the QD method in 1D slab geometry [7]. To obtain the solution of an infinite-medium problem with heterogeneous material composition, we formulate an equivalent finite-medium problem with periodic boundary conditions and generate its solution numerically. This solution is used to linearize the equations of the QD method. These studies showed that the QD method is stable and converges fast on this class of problems in 1D slab geometry. The numerical results showed that the theoretical analysis predicts well the convergence rates of the QD method in the vicinity of the solution. Note that this analysis enabled us to find and predict some

*Current address: AREVA NP Inc., Richland, WA 99352, adrian.constantinescu@areva.com

effects in convergence behavior of the QD method that could not be obtained from either studying the QD method in homogeneous-medium problems or analysis of its linear version on heterogeneous problems. In this paper, we analyze the QD method on 2D problems.

The remainder of this paper is organized as follows. In Sec. 2, the QD method is formulated. The linearization of the discretized 2D QD equations is presented in Sec. 3. In Sec. 4, we describe the Fourier analysis. The numerical results are presented in Sec. 5. In Sec. 6, we conclude with a discussion on the obtained results of analysis of the QD method in 2D.

2. FORMULATION OF THE QD METHOD

We consider a one group transport problem with isotropic scattering and source in 2D Cartesian geometry ($0 \leq x \leq X$, $0 \leq y \leq Y$). The QD method is defined by [5]:

$$\Omega_x \frac{\partial}{\partial x} \psi^{(s+1/2)}(\vec{r}, \vec{\Omega}) + \Omega_y \frac{\partial}{\partial y} \psi^{(s+1/2)}(\vec{r}, \vec{\Omega}) + \sigma_t(\vec{r}) \psi^{(s+1/2)}(\vec{r}, \vec{\Omega}) = \frac{1}{4\pi} \sigma_s(\vec{r}) \phi^{(s)}(\vec{r}) + \frac{1}{4\pi} Q(\vec{r}), \quad (1)$$

$$E_{\alpha\beta}^{(s+1/2)}(\vec{r}) = \int_{4\pi} \Omega_\alpha \Omega_\beta \psi^{(s+1/2)}(\vec{r}, \vec{\Omega}) d\vec{\Omega} \bigg/ \int_{4\pi} \psi^{(s+1/2)}(\vec{r}, \vec{\Omega}) d\vec{\Omega}, \quad \alpha, \beta = x, y, \quad (2)$$

$$\vec{\nabla} \cdot \vec{J}^{(s+1)}(\vec{r}) + \sigma_a(\vec{r}) \phi^{(s+1)}(\vec{r}) = Q(\vec{r}), \quad (3)$$

$$\frac{\partial}{\partial x} \left(E_{xx}^{(s+1/2)}(\vec{r}) \phi^{(s+1)}(\vec{r}) \right) + \frac{\partial}{\partial y} \left(E_{xy}^{(s+1/2)}(\vec{r}) \phi^{(s+1)}(\vec{r}) \right) + \sigma_t(\vec{r}) J_x^{(s+1)}(\vec{r}) = 0, \quad (4)$$

$$\frac{\partial}{\partial x} \left(E_{xy}^{(s+1/2)}(\vec{r}) \phi^{(s+1)}(\vec{r}) \right) + \frac{\partial}{\partial y} \left(E_{yy}^{(s+1/2)}(\vec{r}) \phi^{(s+1)}(\vec{r}) \right) + \sigma_t(\vec{r}) J_y^{(s+1)}(\vec{r}) = 0, \quad (5)$$

and corresponding boundary conditions. Here s is the iteration index. Standard notations are used.

3. LINEARIZATION OF THE DISCRETIZED QD EQUATIONS

We consider rectangular spatial grids $\{x_{i-1/2}, 1 \leq i \leq N_x+1, y_{j-1/2}, 1 \leq j \leq N_y+1\}$. The low-order QD equations (LOQD) (3)-(5) are discretized with a finite volume method [8, 9] and have the following form:

$$\left(J_{x,i+1/2,j}^{(s+1)} - J_{x,i-1/2,j}^{(s+1)} \right) \Delta y_j + \left(J_{x,i,j+1/2}^{(s+1)} - J_{x,i,j-1/2}^{(s+1)} \right) \Delta x_i + \sigma_{a,i,j} \Delta x_i \Delta y_j \phi_{i,j}^{(s+1)} = Q_{i,j} \Delta x_i \Delta y_j, \quad (6)$$

$$\begin{aligned} & \left(E_{xx,i,j}^{(s+1/2)} \phi_{i,j}^{(s+1)} - E_{xx,i-1/2,j}^{(s+1/2)} \phi_{i-1/2,j}^{(s+1)} \right) \Delta y_j \\ & - \left(E_{xy,i,j+1/2}^{(s+1/2)} \phi_{i,j+1/2}^{(s+1)} - E_{xy,i,j-1/2}^{(s+1/2)} \phi_{i,j-1/2}^{(s+1)} \right) \frac{\Delta x_i}{2} + \frac{1}{2} \sigma_{t,i,j} \Delta x_i \Delta y_j J_{i-1/2,j}^{(s+1)} = 0, \end{aligned} \quad (7)$$

$$\begin{aligned} & \left(E_{xx,i+1/2,j}^{(s+1/2)} \phi_{i+1/2,j}^{(s+1)} - E_{xx,i,j}^{(s+1/2)} \phi_{i,j}^{(s+1)} \right) \Delta y_j \\ & - \left(E_{xy,i,j+1/2}^{(s+1/2)} \phi_{i,j+1/2}^{(s+1)} - E_{xy,i,j-1/2}^{(s+1/2)} \phi_{i,j-1/2}^{(s+1)} \right) \frac{\Delta x_i}{2} + \frac{1}{2} \sigma_{t,i,j} \Delta x_i \Delta y_j J_{i+1/2,j}^{(s+1)} = 0, \end{aligned} \quad (8)$$

$$\begin{aligned} & \left(E_{yy,i,j}^{(s+1/2)} \phi_{i,j}^{(s+1)} - E_{yy,i,j-1/2}^{(s+1/2)} \phi_{i,j-1/2}^{(s+1)} \right) \Delta x_i \\ & - \left(E_{xy,i+1/2,j}^{(s+1/2)} \phi_{i+1/2,j}^{(s+1)} - E_{xy,i-1/2,j}^{(s+1/2)} \phi_{i-1/2,j}^{(s+1)} \right) \frac{\Delta y_j}{2} + \frac{1}{2} \sigma_{t,i,j} \Delta x_i \Delta y_j J_{i,j-1/2}^{(s+1)} = 0, \end{aligned} \quad (9)$$

$$\begin{aligned} & \left(E_{yy,i,j+1/2}^{(s+1/2)} \phi_{i,j+1/2}^{(s+1)} - E_{yy,i,j}^{(s+1/2)} \phi_{i,j}^{(s+1)} \right) \Delta x_i \\ & - \left(E_{xy,i+1/2,j}^{(s+1/2)} \phi_{i+1/2,j}^{(s+1)} - E_{xy,i-1/2,j}^{(s+1/2)} \phi_{i-1/2,j}^{(s+1)} \right) \frac{\Delta y_j}{2} + \frac{1}{2} \sigma_{t,i,j} \Delta x_i \Delta y_j J_{i,j+1/2}^{(s+1)} = 0, \end{aligned} \quad (10)$$

$$\Delta x_i = x_{i+1/2} - x_{i-1/2}, \quad \Delta y_j = y_{j+1/2} - y_{j-1/2}.$$

The transport equation (1) is approximated by the method of short characteristics [10–12]. The edge- and cell-average $E_{\alpha\beta}$ are calculated as arithmetic average of vertex values

$$E_{\alpha\beta,i+1/2,j+1/2}^{(s+1/2)} = \sum_m \Omega_{\alpha,m} \Omega_{\beta,m} \psi_{m,i+1/2,j+1/2}^{(s+1/2)} w_m / \sum_m \psi_{m,i+1/2,j+1/2}^{(s+1/2)} w_m, \quad \alpha, \beta = x, y, \quad (11)$$

where w_m is a quadrature weight that corresponds to the discrete ordinates direction $\vec{\Omega}_m$.

To study the convergence behavior of the nonlinear QD method, we linearize the equations in the vicinity of the solution. Assuming that the solution on s -th iteration is close to the converged one, we define

$$\psi_{m,i,j}^{(s+1/2)} = \psi_{m,i,j} + \delta\psi_{m,i,j}^{(s+1/2)}, \quad (12)$$

$$\psi_{m,i+1/2,j}^{(s+1/2)} = \psi_{m,i+1/2,j} + \delta\psi_{m,i+1/2,j}^{(s+1/2)}, \quad (13)$$

$$\psi_{m,i,j+1/2}^{(s+1/2)} = \psi_{m,i,j+1/2} + \delta\psi_{m,i,j+1/2}^{(s+1/2)}, \quad (14)$$

$$\phi_{i,j}^{(s)} = \phi_{i,j} + \delta\phi_{i,j}^{(s)}, \quad (15)$$

$$\phi_{i+1/2,j}^{(s)} = \phi_{i+1/2,j} + \delta\phi_{i+1/2,j}^{(s)}, \quad (16)$$

$$\phi_{i,j+1/2}^{(s)} = \phi_{i,j+1/2} + \delta\phi_{i,j+1/2}^{(s)}. \quad (17)$$

We introduce Eqs. (12)-(17) into the discretized transport and LOQD equations. The linearized LOQD equations can be reduced to the equation for the errors of cell-average scalar fluxes $\delta\phi^{(s)}$

$$\begin{aligned} & \frac{E_{xx,i,j} \delta\phi_{i,j}^{(s+1)} - E_{xx,i+1,j} \delta\phi_{i+1,j}^{(s+1)}}{\sigma_{t,i+1/2,j} \Delta x_i \Delta x_{i+1/2}} - \frac{E_{xx,i-1,j} \delta\phi_{i-1,j}^{(s+1)} - E_{xx,i,j} \delta\phi_{i,j}^{(s+1)}}{\sigma_{t,i-1/2,j} \Delta x_i \Delta x_{i-1/2}} \\ & + \frac{E_{yy,i,j} \delta\phi_{i,j}^{(s+1)} - E_{yy,i,j+1} \delta\phi_{i,j+1}^{(s+1)}}{\sigma_{t,i,j+1/2} \Delta y_j \Delta y_{j+1/2}} - \frac{E_{yy,i,j-1} \delta\phi_{i,j-1}^{(s+1)} - E_{yy,i,j} \delta\phi_{i,j}^{(s+1)}}{\sigma_{t,i,j-1/2} \Delta y_j \Delta y_{j-1/2}} + \sigma_{a,i,j} \delta\phi_{i,j}^{(s+1)} \\ & = - \frac{R_{i+1,j} \delta T_{xx,i+1,j}^{(s+1/2)} - R_{i,j} \delta T_{xx,i,j}^{(s+1/2)}}{\sigma_{t,i+1/2,j} \Delta x_{i+1} \Delta x_{i+1/2}} - \frac{R_{i,j+1/2} \delta T_{xy,i,j+1/2}^{(s+1/2)} - R_{i,j-1/2} \delta T_{xy,i,j-1/2}^{(s+1/2)}}{2\sigma_{t,i+1/2,j} \Delta y_j \Delta x_{i+1/2}} \\ & \quad - \frac{\Delta x_{i+1}}{2\Delta x_i \Delta y_j} \frac{R_{i+1,j+1/2} \delta T_{xy,i+1,j+1/2}^{(s+1/2)} - R_{i+1,j-1/2} \delta T_{xy,i+1,j-1/2}^{(s+1/2)}}{\sigma_{t,i+1/2,j} \Delta x_{i+1/2}} \\ & \quad + \frac{R_{i,j} \delta T_{xx,i,j}^{(s+1/2)} - R_{i-1,j} \delta T_{xx,i-1,j}^{(s+1/2)}}{\sigma_{t,i-1/2,j} \Delta x_i \Delta x_{i-1/2}} + \frac{R_{i,j+1/2} \delta T_{xy,i,j+1/2}^{(s+1/2)} - R_{i,j-1/2} \delta T_{xy,i,j-1/2}^{(s+1/2)}}{2\sigma_{t,i-1/2,j} \Delta y_j \Delta x_{i-1/2}} \\ & \quad + \frac{\Delta x_{i-1}}{2\Delta x_i \Delta y_j} \frac{R_{i-1,j+1/2} \delta T_{xy,i-1,j+1/2}^{(s+1/2)} - R_{i-1,j-1/2} \delta T_{xy,i-1,j-1/2}^{(s+1/2)}}{\sigma_{t,i-1/2,j} \Delta x_{i-1/2}} \\ & \quad - \frac{R_{i,j+1} \delta T_{yy,i,j+1}^{(s+1/2)} - R_{i,j} \delta T_{yy,i,j}^{(s+1/2)}}{\sigma_{t,i,j+1/2} \Delta y_j \Delta y_{j+1/2}} - \frac{R_{i+1/2,j} \delta T_{yx,i+1/2,j}^{(s+1/2)} - R_{i-1/2,j} \delta T_{yx,i-1/2,j}^{(s+1/2)}}{2\sigma_{t,i,j-1/2} \Delta x_i \Delta y_{j-1/2}} \\ & \quad - \frac{\Delta y_{j+1}}{2\Delta x_i \Delta y_j} \frac{R_{i+1/2,j+1} \delta T_{yx,i+1/2,j+1}^{(s+1/2)} - R_{i-1/2,j+1} \delta T_{yx,i-1/2,j+1}^{(s+1/2)}}{\sigma_{t,i,j+1/2} \Delta y_{j+1/2}} \\ & \quad + \frac{R_{i,j} \delta T_{yy,i,j}^{(s+1/2)} - R_{i,j-1} \delta T_{yy,i,j-1}^{(s+1/2)}}{\Delta y_j \Delta y_{j-1/2} \sigma_{t,i,j-1/2}} + \frac{R_{i+1/2,j} \delta T_{yx,i+1/2,j}^{(s+1/2)} - R_{i-1/2,j} \delta T_{yx,i-1/2,j}^{(s+1/2)}}{2\sigma_{t,i,j+1/2} \Delta x_i \Delta y_{j+1/2}} \\ & \quad + \frac{\Delta y_{j-1}}{2\Delta x_i \Delta y_j} \frac{R_{i+1/2,j-1} \delta T_{yx,i+1/2,j-1}^{(s+1/2)} - R_{i-1/2,j-1} \delta T_{yx,i-1/2,j-1}^{(s+1/2)}}{\sigma_{t,i,j-1/2} \Delta y_{j-1/2}}, \end{aligned} \quad (18)$$

$$\sigma_{t,i+1/2,j} = \frac{\sigma_{t,i+1,j} \Delta x_{i+1} + \sigma_{t,i,j} \Delta x_i}{2\Delta x_{i+1/2}}, \quad \Delta x_{i+1/2} = \frac{1}{2}(\Delta x_{i+1} + \Delta x_i),$$

$$\sigma_{t,i,j+1/2} = \frac{\sigma_{t,i,j+1} \Delta y_{j+1} + \sigma_{t,i,j} \Delta y_j}{2\Delta y_{j+1/2}}, \quad \Delta y_{j+1/2} = \frac{1}{2}(\Delta y_{j+1} + \Delta y_j),$$

$$\delta T_{\alpha\beta,i,j}^{s+1/2} = \sum_m (E_{\alpha\beta,i,j} - \Omega_{\alpha,m} \Omega_{\beta,m}) \delta\psi_{m,i,j}^{(s+1/2)} w_m, \quad \alpha, \beta = x, y, \quad (19)$$

$$R_{i,j} = \frac{\phi_{i,j}}{\phi_{i,j}^*}, \quad R_{i,j+1/2} = \frac{\phi_{i,j+1/2}}{\phi_{i,j+1/2}^*}, \quad R_{i+1/2,j} = \frac{\phi_{i+1/2,j}}{\phi_{i+1/2,j}^*}. \quad (20)$$

Here $\phi_{l,p}$ is the solution of the low-order problem, $\phi_{l,p}^*$ is the solution of the high-order problem, $E_{\alpha\beta,i,j}$ is the QD factor calculated by the solution of the transport equation. Note that $\phi_{i,j} \neq \phi_{i,j}^*$ because we use independent discretization of the transport and LOQD equations.

4. FOURIER ANALYSIS

We perform a Fourier analysis for Periodic Horizontal Interface (PHI) problems [1] in a medium that is spatially periodic in y-direction and formed by repeated layers of two different materials with cross sections $\sigma_{t,1}$ and $\sigma_{t,2}$, widths h_1 and h_2 , and equal scattering ratios $c_1 = c_2 = c$. The size of the cell edge in y-direction (Δy_j) is equal to the width of a horizontal material layer. To generate the numerical solution necessary for the stability analysis of a given infinite-medium problem, we solve an equivalent finite-medium problem with just two material layers, 1×2 spatial grid and periodic boundary conditions. This enables us to calculate the infinite-medium solution ($\phi_{l,p}$, $\phi_{l,p}^*$ and $E_{\alpha\beta,i,j}$) which is necessary for linearization.

We now introduce the following Fourier mode ansatz:

$$\delta\psi_{m,i-1/2,j-1/2+2k}^{(s+1/2)} = \omega^s a_{m,j} e^{\hat{i}(\lambda_x x_{i-1/2} + \lambda_y y_{j-1/2+2k})}, \quad (21)$$

$$\delta\phi_{i,j+2k}^{(s)} = \omega^s A_j e^{\hat{i}(\lambda_x x_i + \lambda_y y_{j+2k})}, \quad (22)$$

$$x_i = \frac{1}{2}(x_{i-1/2} + x_{i+1/2}), \quad y_j = \frac{1}{2}(y_{j-1/2} + y_{j+1/2}).$$

$$y_{j+2k} = y_j + k(h_1 + h_2)$$

$$j = 1, 2, \quad k = 0, \pm 1, \pm 2, \dots, \quad \hat{i} = \sqrt{-1},$$

then substitute Eqs. (21)-(22) into the discretized QD equations linearized about the infinite-medium solution and solve for the eigenvalue ω . The spectral radius is defined by $\rho = \sup_{\lambda} |\omega(\lambda)|$.

5. NUMERICAL RESULTS

The results of the Fourier analysis are utilized to evaluate spectral radii for various combinations of layers with different material properties. The predictions based on infinite-medium problems are compared with the results of numerical tests in finite media with a periodic structure, constant source everywhere and vacuum boundary conditions. A product quadrature set with 16 directions per octant was used in all calculations. Table I presents theoretical estimates of the spectral radius, ρ_{th} , versus $\sigma_{t,1}$ and $\sigma_{t,2}$ for $c = 0.9999$, $\Delta x = 1$, $\Delta y_1 = \Delta y_2 = 1$. We notice that the theoretical analysis in infinite media predicts that the QD method loses its effectiveness and even diverges for certain combinations of $\sigma_{t,1}$ and $\sigma_{t,2}$.

The results of the Fourier analysis of the QD method for PHI problems are obtained under the following several assumptions:

1. There is no leakage.
2. There are infinite number of spatial cells. This assumption is especially important for the x-direction for which no conditions are imposed on error modes.
3. The exact solution is the same everywhere in the sense that it is exactly periodic in any location.

However, when one considers finite-medium problems with periodic configurations and non-periodic boundary conditions, the convergence rate will be influenced by the leakage effects near boundaries. These effects destroy perfect periodicity of the solution. As a result, the solution used to perform theoretical

analysis does not exactly match the finite-medium solution. The theoretical results can be rather sensitive to the solution around which the nonlinear equations are linearized. The QD method is a nonlinear one, and a special effort must be made to measure the spectral radius in the vicinity of the solution while performing calculations with finite precision arithmetic. The finite number on cells, for example, along horizontal layers (i.e. in x-direction) eliminates part on errors modes that were accounted for in the infinite-medium analysis. All these effects cause the discrepancy between theoretical and numerical results. The value of the Fourier analysis is that it can show what happens if one considers a problem that meets close enough the above assumptions and what one should expect while approaching this limit.

We now present numerical results for a PHI problem in the square region $\{0 \leq x, y \leq 40\}$ with $c=0.9999$, source $Q = 1$ in the whole domain, and vacuum boundary conditions. Table II shows the spectral radii evaluated in L_2 -norm. The theoretically and numerically estimated spectral radii as functions of $\sigma_{t,2}$ for different $\sigma_{t,1}$ are also plotted in Figure 1. The graphs provide an illustration that help one to correlate the infinite-medium theory with numerical results. For the given set of parameters of transport problems, theoretical results $\rho_{th}(\sigma_{t,1}, \sigma_{t,2})$ give very good qualitative prediction reproducing the shape of numerically estimated spectral radius $\rho_{num}(\sigma_{t,1}, \sigma_{t,2})$ for $\sigma_{t,2} \geq 10^{-1}$. In many cases, the values of ρ_{th} are close to ρ_{num} and provide good estimation of convergence rates in the considered finite-medium problems. The presented numerical results show that the convergence of the QD method slows down if σ_t of layers are significantly different from each other. For example, it happens when $\sigma_{t,1} = 10^4$ and $\sigma_{t,2} = 10^{-1}$. Figure 2 presents theoretically and numerically evaluated ρ for $\sigma_{t,1} = 10^{-1}$ and various scattering ratios. We notice that the QD method exhibits similar effect in case of smaller scattering ratios as well. There are cases in which ρ_{num} is close to the values of the scattering ratio. Thus, we do observe the loss of effectiveness of the QD method in this set of problems with spatial domain $\{0 \leq x, y \leq 40\}$. However, we did not encounter the phenomena of divergence in these finite-medium problems.

To demonstrate finite-medium problems in which the performance of the QD method degrades more dramatically as it predicted by infinite-medium analysis, we consider PHI test problems with significantly larger horizontal dimensions and number of cells in x-direction and fewer number of horizontal layers. We use the same sizes of cells and widths of layers as in the above PHI problems (i.e. $\Delta x = 1$, $\Delta y_1 = \Delta y_2 = 1$). Tables III and IV present the numerically estimated spectral radii in problems with rectangular domains $\{0 \leq x \leq 400, 0 \leq y \leq 12\}$ and $\{0 \leq x \leq 2000, 0 \leq y \leq 4\}$, respectively. Figure 1 shows also graphs of ρ_{num} for these problems.

In the case with 400×12 domain, the numerical results are in much better consistency with the theoretical prediction then the results of problems with 40×40 domain. We now observe the divergence of the QD method, $\rho_{num} > 1$ when $\sigma_{t,1} = 10^4$ and $10^{-2} \leq \sigma_{t,2} \leq 10^{-1}$. The problem with 2000×4 domain has just few horizontal layers and as a result ρ_{num} is far less than ρ_{th} when the optical thickness of the domain in y-direction is small, namely, for $1 \leq \sigma_{t,1} \leq 10^2$ and $10^{-4} \leq \sigma_{t,2} \leq 10^{-1}$. In most of other cases (for example, $\sigma_{t,1} = 10^3$), it is in a good agreement with theoretical estimations. We also notice that the QD method loses its effectiveness and even diverges, for instance, when $10^3 \leq \sigma_{t,1} \leq 10^4$ and $10^{-3} \leq \sigma_{t,2} \leq 10^{-1}$.

The essential feature of the above transport problems is the existence of a long horizontal layer of the same material. The infinite-medium PHI problem is basically a 1D transport problem in which the error modes in x-direction are not synchronized. To eliminate this feature and analyze the behavior of the QD method on a more typical 2D problem, we consider the transport problem with a checker-board configuration of two different materials with $c = 0.9999$ in the square region $\{0 \leq x, y \leq 40\}$. Each material zone is 1×1 . There is one cell per zone. The unit source is defined in the whole domain. Boundary conditions are

vacuum. Table V contains numerically evaluated spectral radii. These results are plotted in Figure 3. In this test, the QD method converges fast in strongly heterogeneous problems for any combination of materials. The spectral radius reaches its maximum value of 0.239 in the case $\sigma_{t,1} = 10^{-2}$ and $\sigma_{t,2} = 10$.

To present the performance of the QD method in problems with heterogeneous media and non-periodic configuration, we show the results of a two-region test problem [4] in the square region $\{0 \leq x, y \leq 40\}$ having $\sigma_{t,1}$ and $Q=1$ for $\{10 \leq x, y \leq 30\}$ and $\sigma_{t,2}$ and $Q=0$ outside of this inner region. The scattering ratio is the same in both regions and $c=0.9999$. The spatial grid is uniform with 40×40 cells. The numerically estimated spectral radii are listed in Table VI and plotted on Figure 4. In this test, the QD method exhibits slowing down of convergence for some set of cross sections. The maximum of ρ occurs for $\sigma_{t,1} = 10^{-2}$ and $\sigma_{t,2} = 10$ and equals 0.46.

6. CONCLUSIONS

We have developed stability analysis of the nonlinear quasidiffusion method for infinite-medium problems with spatially periodic configurations of materials in 2D geometry. This theoretical analysis enabled us to study the convergence properties of the QD method in the vicinity of the solution for problems with periodic horizontal interface and learn about the influence of heterogeneity of the medium on the method convergence. It showed the loss of effectiveness and divergence of the QD method with the considered independent discretization in case of PHI problems consisted of layers with significantly different cross sections. The numerical results confirmed these theoretical predictions. Note that the effectiveness of the DSA method degrades but it still converges. The TSA method diverges for a wide range of parameters of heterogeneous problems. The divergence of the QD method in PHI problems occurs for rather small range of problem parameters. Some additional analysis of the QD method gives us a reason to expect that if the QD equations are discretized consistently, then its behavior will be similar to the one of the DSA method, and it will not diverge.

We now work on further analysis of the QD method for 2D heterogeneous problems and interpretation of the obtained theoretical results. We consider approaches for improving stability properties of the QD method in problems with strong heterogeneities and feasibility of applying Krylov subspace methods for this purpose.

ACKNOWLEDGEMENTS

The work of the second author (DYA) was supported by the Nuclear Engineering Education and Research (NEER) Program of the US Department of Energy under the grant No. DE-FG07-03ID14496.

REFERENCES

- [1] Y. Y. Azmy, "Unconditionally Stable and Robust Adjacent-Cell Diffusive Preconditioning of Weighted-Difference Particle Transport Methods is Impossible," *J. of Comp. Phys.*, **182**, 213-233 (2002).
- [2] J. Chang and M. L. Adams, "Analysis of Transport Synthetic Acceleration for Highly Heterogeneous Problems," *Proc. of M&C Topical Meeting*, Gatlinburg, TN, (2003).

Table I. Theoretically Estimated Spectral Radii of the QD Method for PHI Problem with $c = 0.9999$.

$\sigma_{t,1}$	$\sigma_{t,2}$								
	10^{-4}	10^{-3}	10^{-2}	10^{-1}	1	10^1	10^2	10^3	10^4
1	9.97e-1*	9.84e-1	9.03e-1	5.10e-1	1.94e-1	1.99e-1	2.88e-1	6.36e-1	6.80e-1
10	9.88e-1	9.69e-1	8.95e-1	6.40e-1	1.99e-1	1.63e-1	2.16e-1	4.82e-1	5.44e-1
10^2	7.66e-1	7.41e-1	6.77e-1	5.22e-1	2.88e-1	2.16e-1	9.70e-2	1.06e-1	1.33e-1
10^3	4.93e-1	5.66e-1	1.00e+0	9.12e-1	6.36e-1	4.82e-1	1.06e-1	2.54e-3	1.85e-3
10^4	9.89e-1	1.84E+0	1.69e+0	1.02e+0	6.80e-1	5.44e-1	1.33e-1	1.85e-3	2.59e-5

*Read as 9.97×10^{-1}

Table II. Numerically Estimated Spectral Radii of the QD Method for PHI Problem with $c = 0.9999$ and $\{0 \leq x, y \leq 40\}$.

$\sigma_{t,1}$	$\sigma_{t,2}$								
	10^{-4}	10^{-3}	10^{-2}	10^{-1}	1	10^1	10^2	10^3	10^4
1	7.11e-1	7.03e-1	6.63e-1	4.16e-1	8.64e-2	8.46e-2	1.86e-1	5.58e-1	6.91e-1
10	7.43e-1	7.40e-1	7.16e-1	5.67e-1	8.46e-2	1.23e-1	1.50e-1	4.36e-1	4.96e-1
10^2	4.06e-1	4.13e-1	4.21e-1	3.30e-1	1.86e-1	1.50e-1	6.56e-2	8.67e-2	1.13e-1
10^3	5.96e-2	6.33e-2	1.55e-1	6.51e-1	5.58e-1	4.36e-1	8.67e-2	1.29e-3	1.19e-3
10^4	8.46e-3	6.67e-2	5.17e-1	8.79e-1	6.91e-1	4.96e-1	1.13e-1	1.19e-3	4.79e-6

Table III. Numerically Estimated Spectral Radii of the QD Method for PHI Problem with $c = 0.9999$ and $\{0 \leq x \leq 400, 0 \leq y \leq 12\}$.

$\sigma_{t,1}$	$\sigma_{t,2}$								
	10^{-4}	10^{-3}	10^{-2}	10^{-1}	1	10^1	10^2	10^3	10^4
1	9.24e-1	8.73e-1	7.23e-1	3.13e-1	7.20e-2	1.08e-1	2.11e-1	5.92e-1	6.49e-1
10	9.69e-1	9.48e-1	8.48e-1	5.68e-1	1.08e-1	1.28e-1	1.62e-1	4.38e-1	5.02e-1
10^2	7.16e-1	7.09e-1	6.34e-1	4.58e-1	2.11e-1	1.62e-1	6.92e-2	8.91e-2	1.15e-1
10^3	2.87e-1	3.31e-1	9.59e-1	9.58e-1	5.92e-1	4.38e-1	8.91e-2	1.71e-3	1.19e-3
10^4	1.24e-1	7.88e-1	1.05e+0	1.04e+0	6.49e-1	5.02e-1	1.15e-1	1.19e-3	4.79e-6

Table IV. Numerically Estimated Spectral Radii of the QD Method for PHI Problem with $c = 0.9999$ and $\{0 \leq x \leq 2000, 0 \leq y \leq 4\}$.

$\sigma_{t,1}$	$\sigma_{t,2}$								
	10^{-4}	10^{-3}	10^{-2}	10^{-1}	1	10^1	10^2	10^3	10^4
1	5.27e-1	4.64e-1	3.54e-1	2.27e-1	1.15e-1	1.53e-1	2.48e-1	5.94e-1	6.54e-1
10	6.20e-1	5.73e-1	4.68e-1	3.25e-1	1.53e-1	1.01e-1	1.78e-1	4.39e-1	5.11e-1
10^2	4.76e-1	4.59e-1	4.08e-1	3.43e-1	2.48e-1	1.78e-1	5.54e-2	8.93e-2	1.21e-1
10^3	3.97e-1	4.25e-1	1.00e+0	9.60e-1	5.94e-1	4.39e-1	8.93e-2	1.66e-3	1.51e-3
10^4	4.21e-1	9.92e-1	1.12e+0	1.10e+0	6.54e-1	5.11e-1	1.21e-1	1.51e-3	4.79e-6

Table V. Numerically Estimated Spectral Radii of the QD Method for the Checker-Board Problem, $c = 0.9999$, and $\{0 \leq x, y \leq 40\}$.

$\sigma_{t,1}$	$\sigma_{t,2}$						
	10^{-2}	10^{-1}	1	10	10^2	10^3	10^4
10^{-2}	1.02e-1	6.22e-2	1.45e-1	2.39e-1	1.73e-1	3.06e-2	6.00e-3
10^{-1}	6.22e-2	2.01e-1	1.53e-1	1.80e-1	1.62e-1	3.67e-2	1.32e-2
1	1.45e-1	1.53e-1	1.20e-1	1.19e-1	1.24e-1	1.74e-2	6.97e-3
10	2.39e-1	1.80e-1	1.19e-1	1.28e-1	1.05e-1	1.20e-1	3.44e-2
10^2	1.73e-1	1.62e-1	1.24e-1	1.05e-1	6.98e-2	2.19e-2	2.92e-3
10^3	3.06e-2	3.67e-2	1.74e-2	1.20e-1	2.19e-2	1.29e-3	2.07e-4
10^4	6.00e-3	1.32e-2	6.97e-3	3.44e-2	2.92e-3	2.07e-4	9.35e-10

Table VI. Numerically Estimated Spectral Radii of the QD Method for the Two-Region Problem with $c = 0.9999$ and $\{0 \leq x, y \leq 40\}$.

$\sigma_{t,1}$	$\sigma_{t,2}$						
	10^{-2}	10^{-1}	1	10	10^2	10^3	10^4
10^{-2}	5.60e-2	1.20e-1	3.98e-1	4.60e-1	3.82e-1	2.70e-1	2.81e-1
10^{-1}	2.53e-1	2.00e-1	2.99e-1	3.41e-1	2.85e-1	3.06e-1	3.22e-1
1	3.91e-1	2.96e-1	8.63e-2	1.58e-1	1.96e-1	2.64e-1	2.68e-1
10	2.50e-1	2.44e-1	1.42e-1	1.22e-1	1.47e-1	2.00e-1	2.14e-1
10^2	1.71e-1	1.51e-1	1.54e-1	1.45e-1	6.55e-2	7.72e-2	8.52e-2
10^3	4.51e-2	2.28e-1	2.08e-1	1.69e-1	8.03e-2	1.29e-3	1.16e-3
10^4	5.16e-2	2.56e-1	2.16e-1	1.73e-1	8.37e-2	2.90e-5	4.79e-6

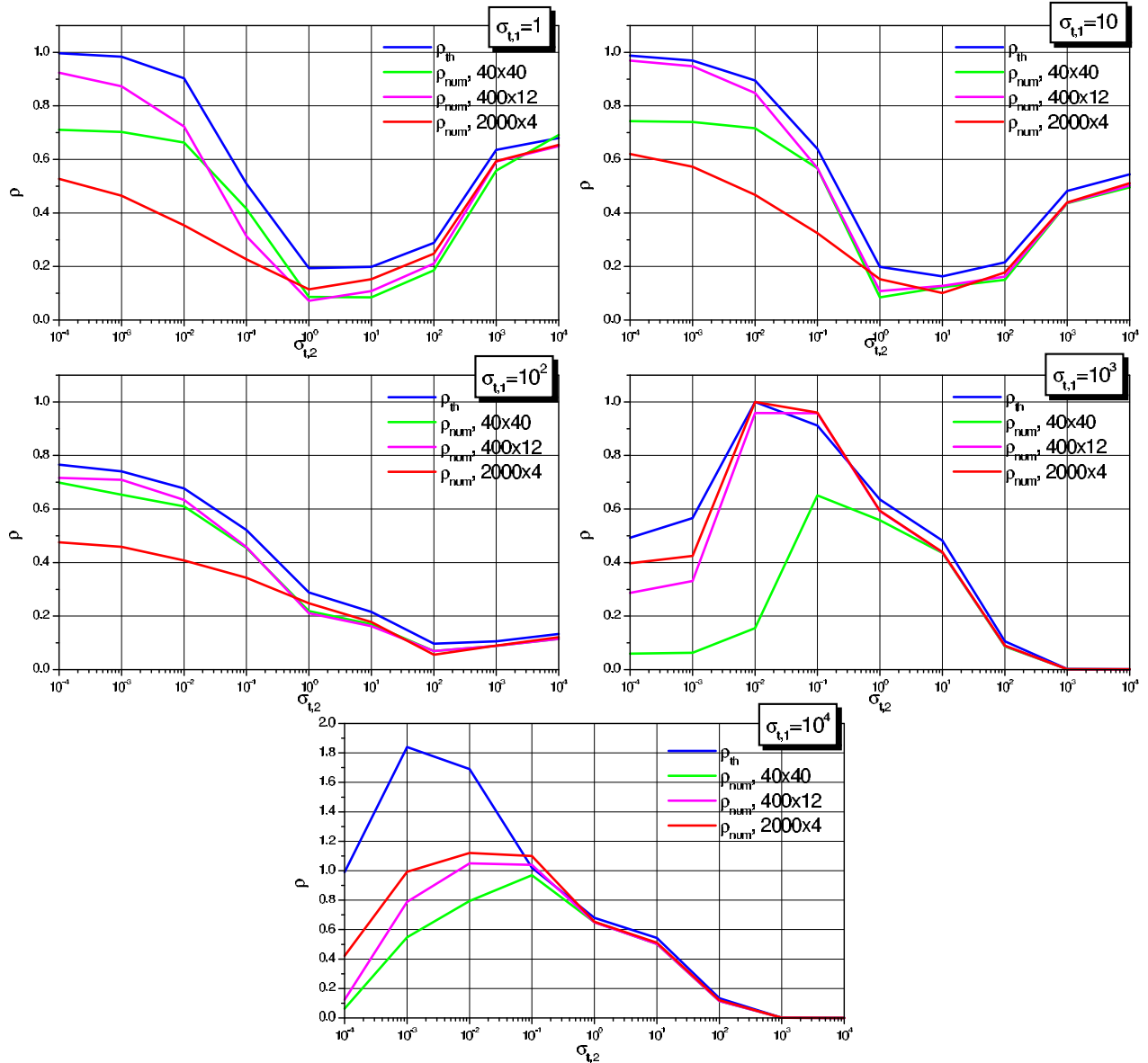


Figure 1. Theoretically (ρ_{th}) and numerically (ρ_{num}) estimated spectral radii of the QD method, $c = 0.9999$.

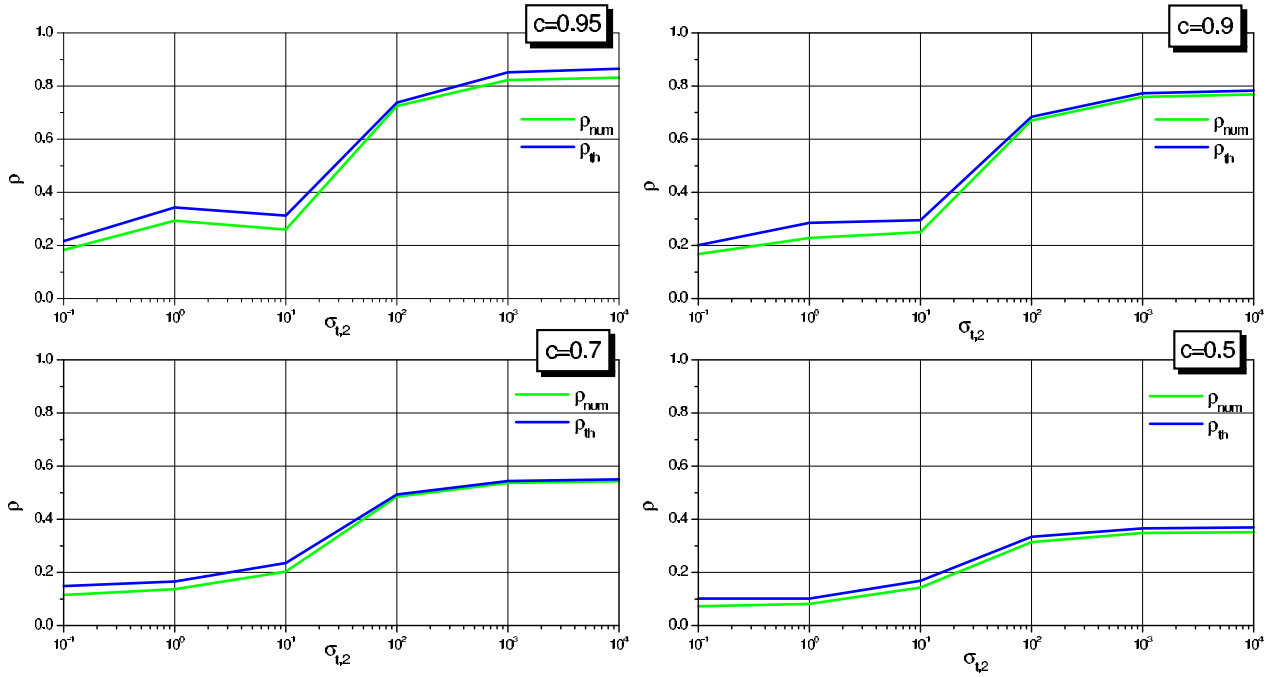


Figure 2. Theoretically (ρ_{th}) and numerically (ρ_{num}) estimated spectral radii of the QD method, $\sigma_{t,1} = 10^{-1}, \{0 \leq x, y \leq 40\}$.

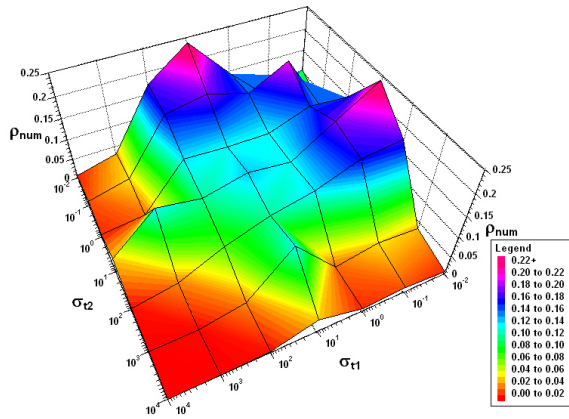


Figure 3. Numerically estimated spectral radii of the QD method for the checker-board problem, $c = 0.9999$.

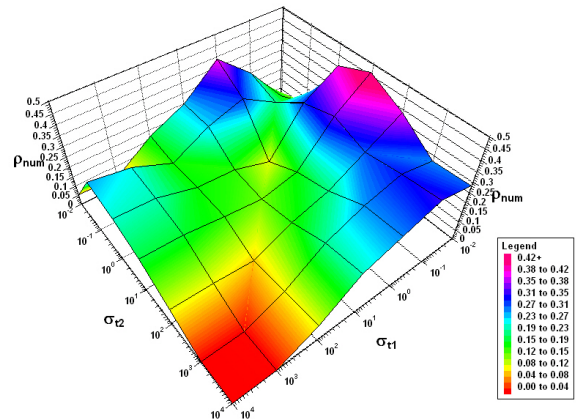


Figure 4. Numerically estimated spectral radii of the QD method for the two-region problem with $c = 0.9999$.

- [3] R. Sanchez, "On the Spectral Analysis of Iterative Solutions of the Discretized One-Group Transport Equation," *Annals of Nuclear Energy*, **149**, pp. 2059-2075 (2004).
- [4] J. S. Warsa, T. A. Wareing, J. E. Morel, "Krylov Iterative Methods and the Degraded Effectiveness of diffusion Synthetic Acceleration for Multidimensional S_N Calculations in Problems with Material Discontinuities," *Nucl. Sci. Eng.*, **147**, pp. 218-248 (2004).
- [5] V. Ya. Gol'din, "A Quasi-Diffusion Method of Solving the Kinetic Equation," *USSR Comp. Math. and Math. Phys.*, **4**, 136-149 (1964).
- [6] G. R. Cefus and E. W. Larsen, "Stability Analysis of the Quasidiffusion and Second Moment Methods for Iteratively Solving Discrete-Ordinates Problems," *Transp. Theory & Stat. Phys.*, **18**, 493-511 (1989-90).
- [7] A. Constantinescu and D.Y. Anistratov, "Stability Analysis of the Quasidiffusion Method for 1D Periodic Heterogeneous Problems," *Trans. Am. Nucl. Soc.*, **95**, 2006.
- [8] E.N.Aristova, V.Ya. Gol'din, and A.V.Kolpakov, "Multidimensional Calculations of Radiation Transport by Nonlinear Quasi-Diffusion Method," *Proceeding of ANS International Conference on Mathematics and Computation, Reactor Physics and Environmental Analysis in Nuclear Applications*, Sept. 27-30, 1999, Madrid, Spain, 667-676 (1999).
- [9] V.Ya. Gol'din, D. A. Gol'dina and A.V. Kolpakov, "The Solution of Two-Dimensional Stationary Quasidiffusion Problem," *Preprint of the Keldysh Institute for Applied Mathematics*, the USSR Academy of Sciences, No. 49 (1982) (in Russian).
- [10] V.Ya. Gol'din, "Characteristic Difference Scheme for Non-Stationary Kinetic Equation," *Soviet Mathematics - Doklady*, **1**, 902 (1960).
- [11] V.Ya. Gol'din, N.N. Kalitkin, and T.V. Shishova, "Nonlinear Difference Schemes for Hyperbolic Equations," *USSR Comp. Math. and Math. Phys.* **5**, 229 (1968).
- [12] K.Takeuchi, "A Numerical Method for Solving the Neutron Transport Equation in Finite Cylindrical Geometry," *J. Nucl. Sci.*, **6**, 446 (1969).